Cardiac Physiologic and Genetic Predictors of Hyperoxia-Induced Acute Lung Injury in Mice

Reuben Howden[1], Hye-Youn Cho[2], Laura Miller-DeGraff[2], Christopher Walker[2], James A. Clark[3], Page H. Myers[3], D. Clay Rouse[4], and Steven R. Kleeberger[2]

[1]Department of Kinesiology, University of North Carolina at Charlotte, Charlotte, North Carolina; [2]Laboratory of Respiratory Biology, and [3]Comparative Medicine Branch, National Institute of Environmental Health Sciences, National Institutes of Health, Research Triangle Park, North Carolina; and [4]Division of Laboratory Animal Resources, Duke University Medical Center, Durham, North Carolina

Exposure of mice to hyperoxia produces pulmonary toxicity similar to acute lung injury/acute respiratory distress syndrome, but little is known about the interactions within the cardiopulmonary system. This study was designed to characterize the cardiopulmonary response to hyperoxia, and to identify candidate susceptibility genes in mice. Electrocardiogram and ventilatory data were recorded continuously from 4 inbred and 29 recombinant inbred strains during 96 hours of hyperoxia (100% oxygen). Genome-wide linkage analysis was performed in 27 recombinant inbred strains against response time indices (TIs) calculated from each cardiac phenotype. Reductions in minute ventilation, heart rate (HR), low-frequency (LF) HR variability (HRV), high-frequency HRV, and total power HRV were found in all mice during hyperoxia exposure, but the lag time before these changes began was strain dependent. Significant (chromosome 9) or suggestive (chromosomes 3 and 5) quantitative trait loci were identified for the HRTI and LFTI. Functional polymorphisms in several candidate susceptibility genes were identified within the quantitative trait loci and were associated with hyperoxia susceptibility. This is the first study to report highly significant interstrain variation in hyperoxia-induced changes in minute ventilation, HR, and HRV, and to identify polymorphisms in candidate susceptibility genes that associate with cardiac responses. Results indicate that changes in HR and LF HRV could be important predictors of subsequent adverse outcome during hyperoxia exposure, specifically the pathogenesis of acute lung injury. Understanding the genetic mechanisms of these responses may have significant diagnostic clinical value.

Keywords: heart rate; hyperoxia; genome-wide mapping

CLINICAL RELEVANCE

The toxicity of hyperoxia on the pulmonary system is well defined. However, little is known about the cardiac responses to hyperoxia or the genetic component to such effects. Genome-wide linkage analyses identified chromosomal regions and candidate genes for differential susceptibility in heart rate and heart rate variability responses, and provided insights into the genetic mechanisms associated with cardiac responses to hyperoxia. Cardiac responses in a mouse model of acute lung injury may be a useful indicator of adverse pulmonary outcome in response to hyperoxia.

Acute lung injury (ALI), acute respiratory distress syndrome, and bronchopulmonary dysplasia can develop in patients exposed to supplemental oxygen (hyperoxia). Insufficient detoxification of reactive oxygen species allows these oxidants to interact with cellular components and cause pulmonary cell damage or death, tissue and alveolar edema, surfactant dysfunction, lung inflammation, and subsequent deterioration of lung function during hyperoxia exposure (1). Variation in susceptibility to hyperoxia between patients (2) and the extent of hyperoxic lung injury among strains of mice (3, 4) indicates a genetic contribution to these disorders. Effects of exposure (3–5 d) to hyperoxia on rodent lung have been described previously (5), and pulmonary injury susceptibility genes have been determined, including nuclear factor, erythroid derived 2, like 2 (6, 7). However, it is not clear if incomplete detoxification of reactive oxygen species during hyperoxia is localized to the lung or is systemic, involving cardiovascular function.

Hyperoxia-induced perivascular edema and compensatory increases in cardiac output have been reported previously using rabbits (8) and dogs (9). Furthermore, the pulmonary and cardiovascular systems are known to be regulated in "concert" (10), indicating that alterations in cardiovascular function may play a critical role in development of pulmonary morbidity and mortality caused by hyperoxia. It is also well known that central control of cardiovascular and pulmonary systems is coordinated to ensure adequate tissue perfusion for a given aerobic oxygen demand (11). Lung injury induced by smoke inhalation induces hemodynamic and cardiovascular changes (12), and 72 hours of continuous hyperoxia caused a sustained increase in heart rate (HR) and a reduction in blood pressure in rabbits (13). However, the molecular mechanisms of cardiovascular responses to hyperoxia remain unclear.

HR and HR variability (HRV) are established clinical tools for assessing autonomic nervous system function and cardiovascular health (14). Significant changes in HR and HRV are known indicators of cardiovascular risk. However, there is a paucity of data describing the HR and HRV responses to chronic hyperoxia exposure and the effect of genetic background. The first objective of this study was to determine the dynamics of HR and HRV during hyperoxia using inbred strains known to have differential pulmonary susceptibility to hyperoxia. The second objective was to use recombinant inbred (RI) strains of mice to identify quantitative trait loci (QTLs) that determine susceptibility to hyperoxia-induced changes in HR and HRV, and to identify candidate susceptibility genes in the QTLs.

(*Received in original form June 15, 2011 and in final form November 1, 2011*)

This work was supported by the Intramural Research Program of the National Institute of Environmental Health Sciences, National Institutes of Health, Department of Health and Human Services.

Author Contributions: R.H. determined the experimental study design and methodology used, performed functional heart analysis, and drafted the manuscript; H.-Y.C. determined lung injury responses and drafted the manuscript; L.M.-D., C.W., J.A.C., P.H.M., and D.C.R. assisted with the survival surgery and the necropsies; and S.R.K. helped in experimental study design and drafting the manuscript.

Correspondence and requests for reprints should be addressed to Reuben Howden, Ph.D., Department of Kinesiology, University of North Carolina at Charlotte, Charlotte, NC 28223. E-mail: rhowden@uncc.edu

This article has an online supplement, which is accessible from this issue's table of contents at www.atsjournals.org

Am J Respir Cell Mol Biol Vol 46, Iss. 4, pp 470–478, Apr 2012
Published 2012 by the American Thoracic Society
Originally Published in Press as DOI: 10.1165/rcmb.2011-0204OC on November 3, 2011
Internet address: www.atsjournals.org

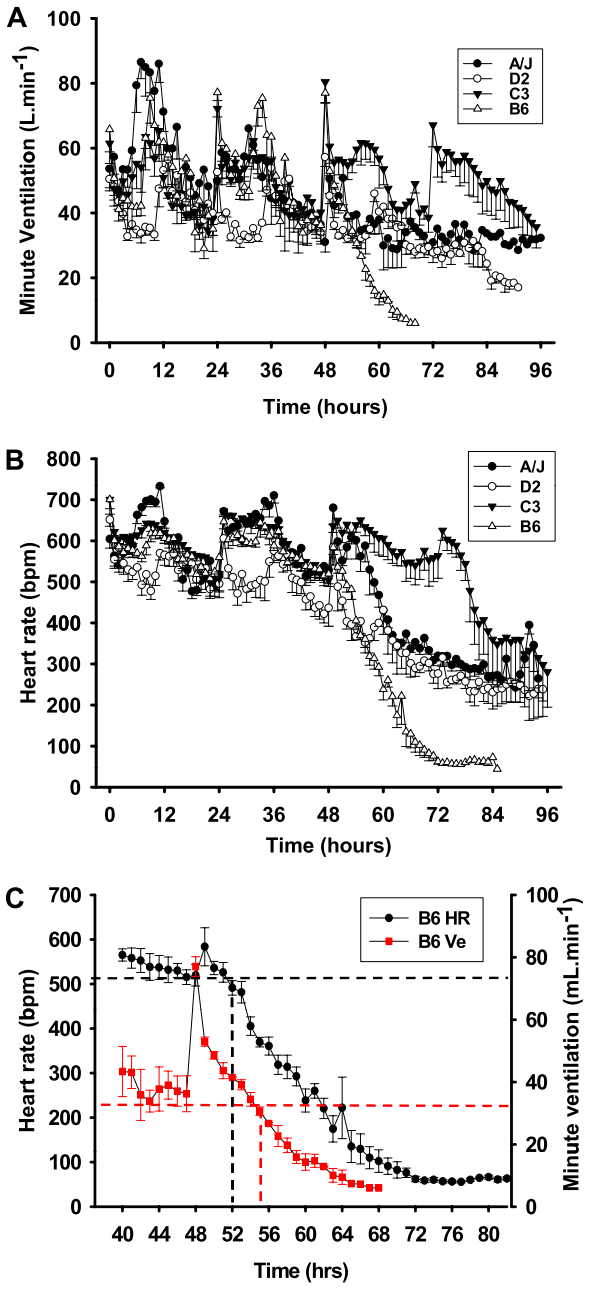

Figure 1. Differential cardiopulmonary response to hyperoxia in four inbred strains of mice. (*A*) Minute ventilation ($\dot{V}_E$) responses to hyperoxia. The acute increases in $\dot{V}_E$ at 24 and 48 hours of exposure were caused by handling of the mice during chamber cleaning. The absence of these changes at 72 hours of exposure was likely due to the effect of hyperoxia on the pulmonary system. Values are means (±SEM) from 20 minutes of pulmonary function data per hour. (*B*) Heart rate (HR) (beats per minute [bpm]) responses to hyperoxia. Values are means (±SEM) from 20 minutes of electrocardiogram (ECG) recording per hour. (*C*) Example data from B6 mice exposed to hyperoxia showing that HR began to decline before $\dot{V}_E$. Values are means (±SEM) from 20 minutes of ECG recording or pulmonary function data per hour ($n = 8$ mice/strain).

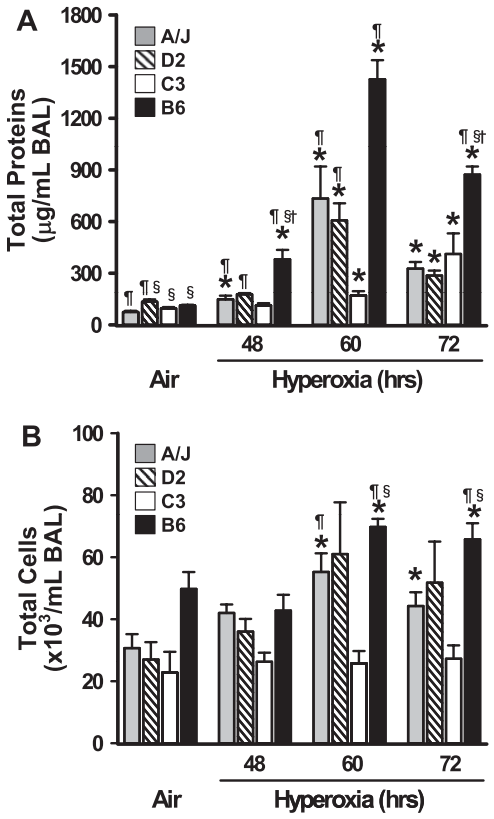

Figure 2. Differential pulmonary protein edema and cellular injury in four inbred strains of mice after hyperoxia exposure. Total protein concentration (*A*) and numbers of total bronchoalveolar lavage (BAL) cells (*B*) were determined by BAL analysis in inbred strains of mice after air or hyperoxia (48, 60, and 72 h) exposure. Data presented as mean (±SEM) (n = 3–8 mice/group). *Significantly different from strain-matched air controls ($P < 0.05$); ¶significantly different from similarly exposed C3H/HeJ (C3) mice ($P < 0.05$); §significantly different from similarly exposed A/J mice; †significantly different from similarly exposed D2 mice ($P < 0.05$). B6, C57BL/6J.

MATERIALS AND METHODS

Animals

A/J, C3H/HeJ (C3), C57BL/6J (B6), DBA/2J (D2), and 29 AXB/BXA RI strains were exposed to hyperoxia (96 h) for cardiopulmonary assessment (Jackson Laboratory, Bar Harbor, ME). AXB and BXA RI mice are inbred F_2 lines derived from A/J and B6 parental strains. Baseline ventilatory and HR measurements on the AXBXA RI mice were published previously (15). Mice (n = 2–5 per strain [*see* Table E1 in the online supplement for RI strain sample sizes]; 8–21 wk; mean strain body mass, 19.5–38.4 g) were housed with a 12-hour:12-hour light:dark cycle, and food (NIH-31) and water were provided *ad libitum*. Animals were handled in accordance with National Institutes of Health Humane Care and Use of Laboratory Animals guidelines.

Surgical Implantation of Radio Telemetry Transmitter

Implantation procedures for ETA-F20 electrocardiogram (ECG) transmitters (DSI, Arden Hills, MN) are described elsewhere (15). Mice recovered from surgery for 5 days before hyperoxia exposures began. Additional methods are described in the online supplement.

Hyperoxia Exposure and Measurements

Cardiopulmonary function during hyperoxia (100% oxygen to 96 h until moribund or when HR reached ~200 bpm) was assessed after baseline ECG and pulmonary function recording. ECG data were then used to calculate HR and HRV. HRV calculations were made in two frequency ranges. Low-frequency (LF) HRV indicates the level of variation in sympathetic regulation of HR. High-frequency (HF) HRV indicates the level of variation in parasympathetic regulation of HR. Changes in HRV suggest a disturbance in the autonomic nervous system control of the heart. We also calculated total power (TP), which

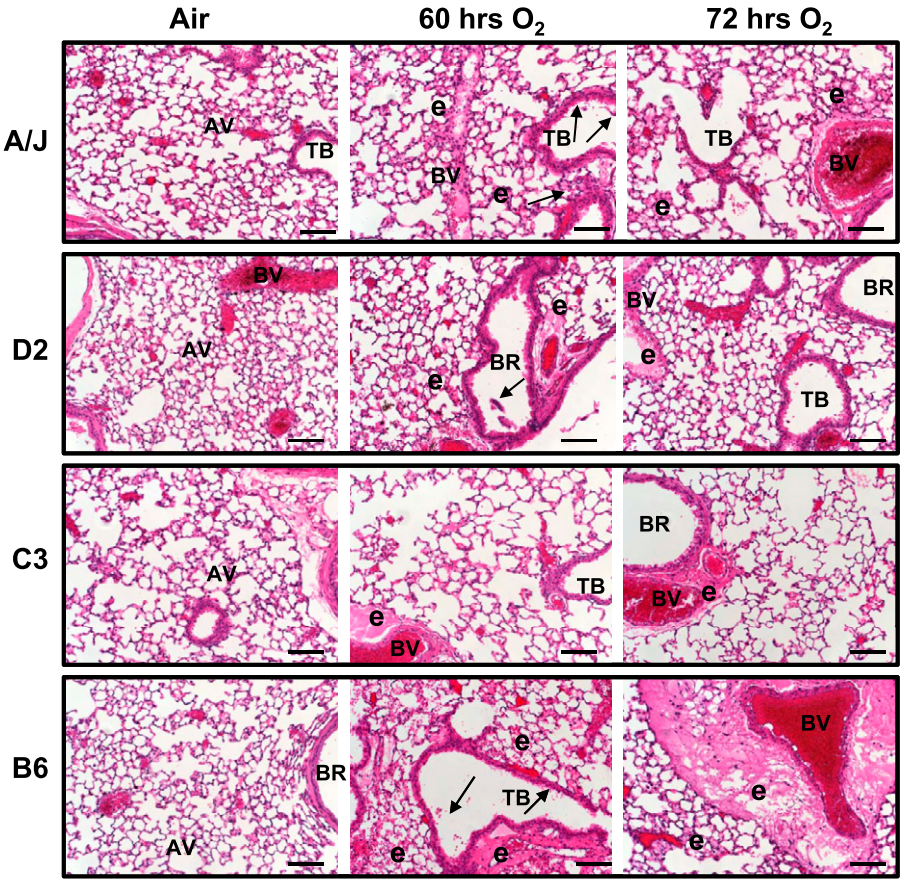

Figure 3. Differential pulmonary histopathology developed after hyperoxia exposure in four inbred strains of mice. Representative light photomicrographs of left lung sections from A/J, DBA/2J (D2), C3H/HeJ (C3), and C57BL/6J (B6) mice (n = 3–5/group) of air controls or hyperoxia (60 and 72 h) stained with H and E. *Arrows* indicate epithelial cell sloughing. AV, alveoli; BR, bronchi or bronchiole; BV, blood vessel; e, alveolar and tissue (perivascular-peribronchiolar) edema; and TB, terminal bronchiole. *Scale bars*, 100 μm.

was a summation of LF and HF as a measure of total HR variation in the frequencies measured. In separate exposures to assess hyperoxia-induced lung injury, inbred mice were exposed continuously to hyperoxia or filtered air for 48, 60, or 72 hours. Procedures for bronchoalveolar lavage (BAL) analysis of the right lung and histopathology of the fixed left lung are described elsewhere (6). Additional methods are described in the online supplement.

Genetic Linkage Analysis

Genome-wide scans for QTLs were performed using RI phenotypes from 27 RI lines and the WebQTL resource (http://www.genenetwork.org), as described previously (15, 16). AXB19a and AXB19b were excluded from the linkage analyses as they are considered sister strains with AXB19 (http://jaxmice.jax.org/jaxnotes/504/504e.html), and thus do not provide additional informative genetic insight. Marker regression analysis was used across the genome at the location of available marker loci using phenotype data from the RI strains. Additional details are described in the online supplement.

Statistical Analysis

For linkage analyses with the RI strains, we quantitated minute ventilation ($\dot{V}_E$), HR, and HRV responses by calculating the area under the curve for each parameter from 40 hours of exposure to the time at which HRs reached 220 bpm. These calculations, or time indices (TIs), are hereafter referred to as $\dot{V}_E$ TI, HRTI, HFTI, LFTI, and TPTI. Higher TIs indicate greater resistance to hyperoxia. Baseline and hyperoxia response phenotype differences between strains were assessed independently using one-way ANOVA (two-tailed) with Student-Newman-Keuls *post hoc* test for pairwise comparisons. Student's t test (two-tailed) was used to test whether single-nucleotide polymorphisms (SNPs) in candidate genes associated with HRTI or LFTI among RI strains. BAL data (n = 3–5/group) are expressed as group means (±SEM). Two-way ANOVA (two-tailed) was used to evaluate effects of exposure (air; 48-, 60-, and 72-h O_2) and strain (A/J, C3, B6, D2) on total protein concentration and cell number.

RESULTS

Inbred Strain Comparison of Cardiopulmonary Phenotypes

$\dot{V}_E$ response to hyperoxia. $\dot{V}_E$ in all strains followed the expected circadian pattern for at least the first 48 hours of hyperoxia (Figure 1A). A significantly greater reduction in $\dot{V}_E$ was observed in D2 mice relative to other inbred strains during diurnal periods when activity was lowest. However, this did not appear to influence hyperoxia susceptibility of this strain.

A consistent and precipitous fall in $\dot{V}_E$ was found in B6 mice after 55 hours of hyperoxia (Figures 1A and 1C). This reduction in $\dot{V}_E$ continued until mice were killed due to moribundity. In other strains, reductions in $\dot{V}_E$ were also observed, but were smaller and occurred later (Figure 1A).

Differential pulmonary protein hyperpermeability and cellular injury in inbred strains. Relative to air controls, 48 hours of hyperoxia caused a small but statistically significant increase in total BAL protein concentrations in A/J and B6 mice (Figure 2A). The hyperoxia-induced increase in BAL protein in B6 mice was significantly greater compared with other strains at 48 hours (Figure 2A). Protein edema developed in all strains after 60 and 72 hours of hyperoxia, and highest BAL protein concentrations were found in B6 mice, whereas protein was lowest in C3 mice (Figure 2A). Similar strain-dependent patterns of response over time were observed for protein hyperpermeability and changes in $\dot{V}_E$ during hyperoxia (Figure 1A)

Total BAL cell numbers were significantly higher in air-exposed B6 mice relative to D2 and C3 mice (Figure 2B).

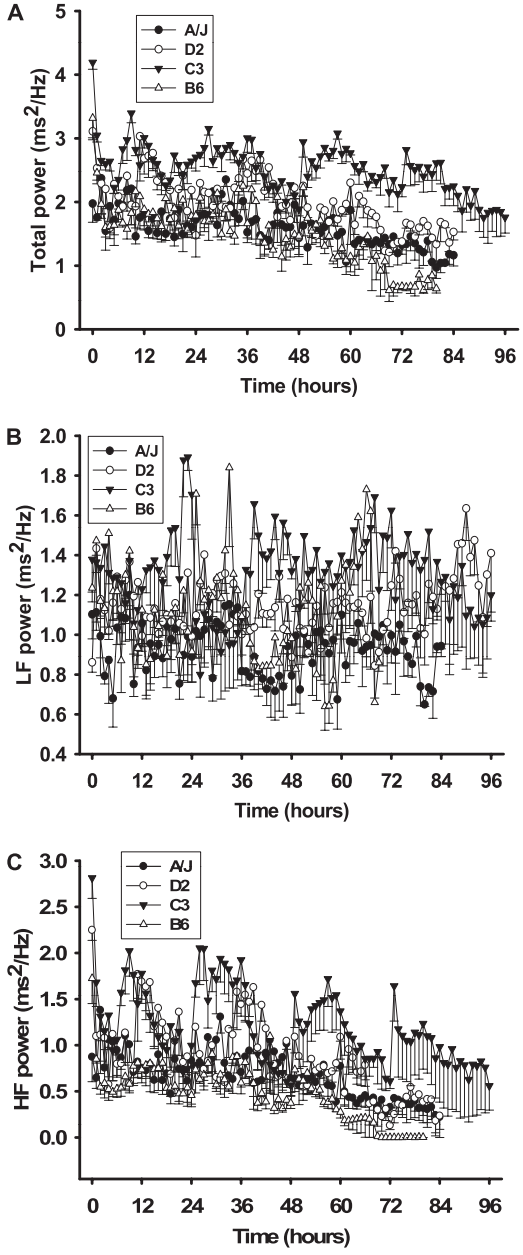

Figure 4. Differential HR variability responses of four inbred strains. (*A*) Total power (TP) responses. TP is the summation of values from the low-frequency (LF) (*B*) and high-frequency (HF) (*C*) ranges acquired from individual mice. All values presented are means (±SEM) from 20 minutes of ECG recording per hour.

Significantly greater numbers of BAL inflammatory cells were found in B6 and D2 mice only after 60 and 72 hours of hyperoxia (Figure 2B). Total BAL cells in C3 mice were significantly lower compared with other strains after 60 and 72 hours of hyperoxia (Figure 2B).

Differential lung histopathology in inbred strains. No histopathological changes were found in lungs of air-exposed mice (Figure 3). Hyperoxia induced exfoliation of epithelial lining from bronchi to terminal bronchioles, and inflammatory cell infiltration was present in all strains, but to a greater degree in A/J and D2 mice. Epithelial cell sloughing accompanied the compensatory hyperplasia. Alveolar vacuolization and loss of alveolar structure (prevalent in A/J mice), perivascular lymphocyte accumulation (prevalent in D2 and C3 mice), and alveolar epithelial hypotrophy or atrophy (C3 mice) were also evident at 60 to 72 hours (Figure 3). The magnitude of peribronchial–perivascular and alveolar edema was much more severe in B6 mice than in other strains, corresponding to the highest BAL protein concentration in these mice (Figure 2A).

HR and HRV in response to hyperoxia. During the first 48 hours of hyperoxia, normal circadian variation in HR was observed in all strains (Figure 1B), similar to that for $\dot{V}_E$. After 49 hours of exposure, a continuous reduction in HR occurred (mean ± SEM, 700.6 ± 22.4 to 44.1 [single mouse] bpm; Figure 1B) for 31 hours in B6 mice (Figures 1B and 1C). Reductions in HR were also found in other inbred strains. HR reductions in D2 mice began at approximately the same time as in B6 mice, but HR response observed in B6 mice progressed more rapidly. The beginning reduction in HR observed in A/J mice was intermediate, but the overall response was almost identical to D2 mice. However, HRs in C3 mice did not begin to reduce until approximately 80 hours of hyperoxia.

Baseline TP was significantly different between all strain pairwise comparisons ($P \geqslant 0.001$), except B6 versus D2 (*see* Figure 4A). Baseline HF was significantly different between strains, except C3 versus D2 and D2 versus B6 ($P \leqslant 0.05$) (Figure 4B). Baseline LF was significantly different between all other inbred strain combinations ($P \leqslant 0.001$), except for D2 versus B6 (Figure 4C).

Hyperoxia-induced reductions in TP were observed in all inbred strains at 1 hour, except for A/J mice. TP was significantly higher during active periods (12, 36, 60, 84 h; Figure 4A) for lung injury–resistant C3 mice than for all other inbred strains. In all other inbred strains, few changes in TP were observed during hyperoxia. LF HRV did not change in a given direction during hyperoxia compared with baseline measures. However, it should be noted that the LFTI was different between B6 and A/J mice (*see below*), and LFTI was used for QTL mapping. In C3 and D2 mice, normal circadian variation was seen during the first 48 hours of hyperoxia (Figure 4B). From 48 to 72 hours, circadian variation was observed in C3 mice only, after which HF become more consistent in these mice, until exposure ended at 96 hours. Minimal circadian changes were found in B6 and A/J mice during the experiment. HF was zero from 70 hours, although this was likely associated with very low HRs seen in these mice.

QTL Mapping with AXB/BXA RI Strains

HR and HRV. A continuous distribution was found for HRTI (Figure 5A), suggesting that multiple genes contribute to this phenotype (range, BXA13 = 5,698.65 ± 943.94 bpm × time and AXB23 = 22,252.87 ± 305.68 bpm × time). Similarly, HRV phenotypes were continuously distributed, and BXA13 mice were most responsive for all components of HRV (Figure 5). TPTI ranged from 24.46 ± 3.75 m^2/Hz × time (AXB20) to 94.13 ± 19.70 m^2/Hz × time (BXA 4), and the RI strain distribution patterns for TPTI and HRTI were similar (Figure 5B). The distribution of HFTI between strains (6.49 ± 2.28 m^2/Hz × time [BXA13] to 30.08 ± 3.50 m^2/Hz × time [BXA4]) was very similar to TPTI, and therefore a large proportion of between strain variation observed in TPTI was attributed to HFTI (Figure 5C). The LFTI was also continuously distributed among strains (Figure 5D). Using a node and edge plot, we found that HR and all HRV phenotypes were significantly correlated with one another during hyperoxia, but HF was the only basal phenotype correlated with hyperoxia responses (Figure 6). Moreover, although basal ventilatory parameters were related to one another as expected, they were not correlated with HR or any HRV phenotypes.

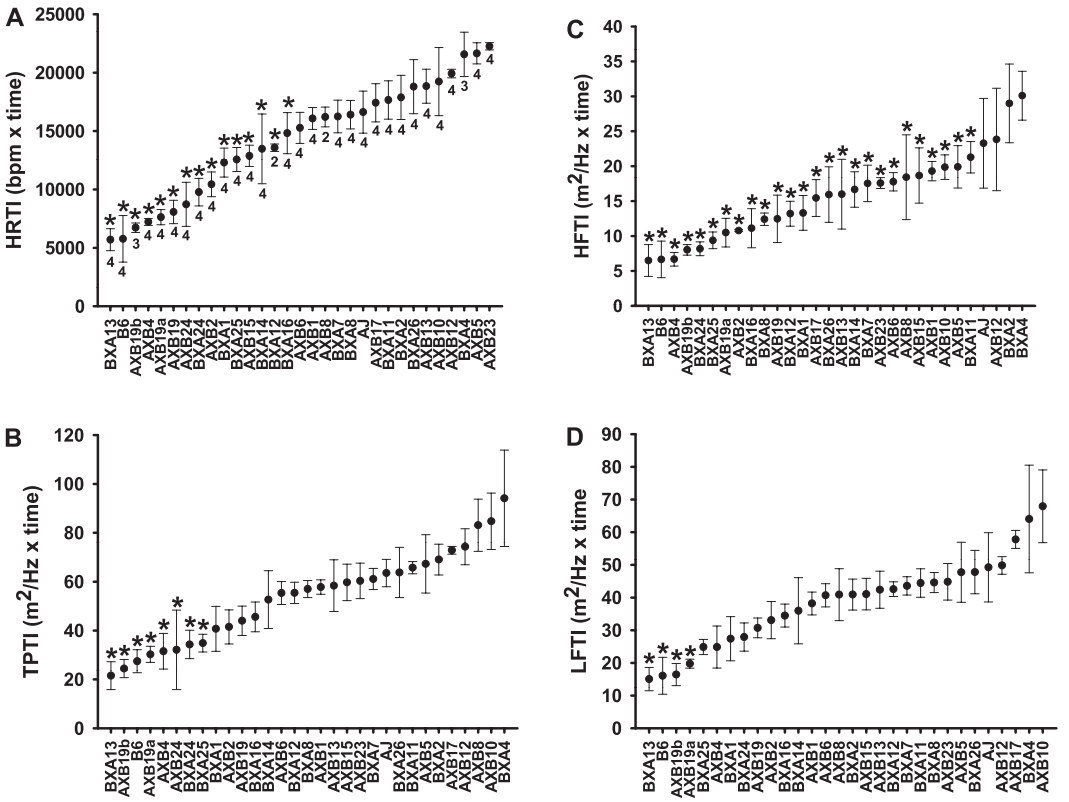

Figure 5. Differential HR and HR variability (HRV) hyperoxia response indices of AXB/BXA recombinant inbred (RI) strains, and B6 and A/J mice. Indices measured are (*A*) HR time index (TI) (HRTI), (*B*) TPTI, (*C*) HFTI, and (*D*) LFTI. Values are the integrated area under the curve for each response from 40 hours of hyperoxia until HR declined to 220 bpm. Means (±SEM) of individual mice in each RI strain are presented. *$P \leq 0.05$ compared with the strain with the highest value in the individual response indices.

Genome-wide scans were performed for basal HR, HRV, and ventilatory phenotypes (15), and hyperoxia-induced changes in HR and HRV phenotypes in RI strains (Figure 7A). The cluster map for all scans is consistent with phenotype relatedness (*see* Figure 6), and regions on chromosomes 3 (suggestive QTL for HRTI), 5 (suggestive QTLs for HRTI and LFTI), and 9 (significant QTLs for HRTI and LFTI; Figure 7B) were most consistently associated with hyperoxia response phenotypes. All of the genes within the significant and suggestive QTL intervals are in Table E2. The significant overlapping QTLs on chromosome 9 were located between 52.3229 and 68.4965 Mbp (Figure 7C, Table 1). We then queried the Mouse Phenome Database (http://phenome.jax.org; Jackson Laboratory) for informative SNPs in genes within the interval to determine whether one or more SNPs significantly associated with HRTI or LFTI among the RI strains. We limited our searches to minor allele SNPs that were present in at least 10% of all strains. A nonsynonymous coding SNP (G/T) was identified that causes an amino acid substitution (Cys265Phe) in exon 8 of timeless interacting protein (*Tipin*), and the HRTI and LFTI responses in RI strains homozygous for the G allele ($n = 10$ strains) were significantly greater than in RI strains with the T allele (16 strains; Table 2). Similarly, a nonsynonymous coding SNP (C/T; Met770Val) in thrombospondin type I, domain containing 4 (*Thsd4*) was significantly associated

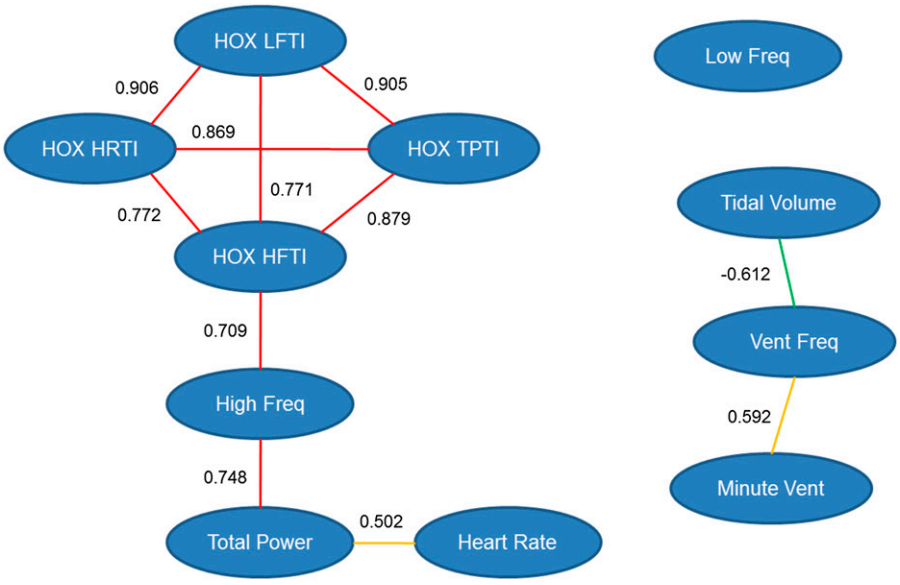

Figure 6. Node and edge plot for association of basal and hyperoxia response phenotypes of AXB/BXA RI strains. HRTI and all HR variability TIs were significantly correlated with one another during exposure to hyperoxia. HF HR variability was the only basal phenotype correlated with the hyperoxia responses. Although the basal ventilatory parameters were related to one another as expected, they were not correlated with HR or any HRV phenotypes. Numbers beside the edges are Pearson correlation coefficients between phenotypes (nodes). Pearson correlation values are represented as: *red edges*, 0.7–1.0; *orange edges*, 0.5–0.7; *green edges*, −0.7 to −0.5. HOX, hyperoxia.

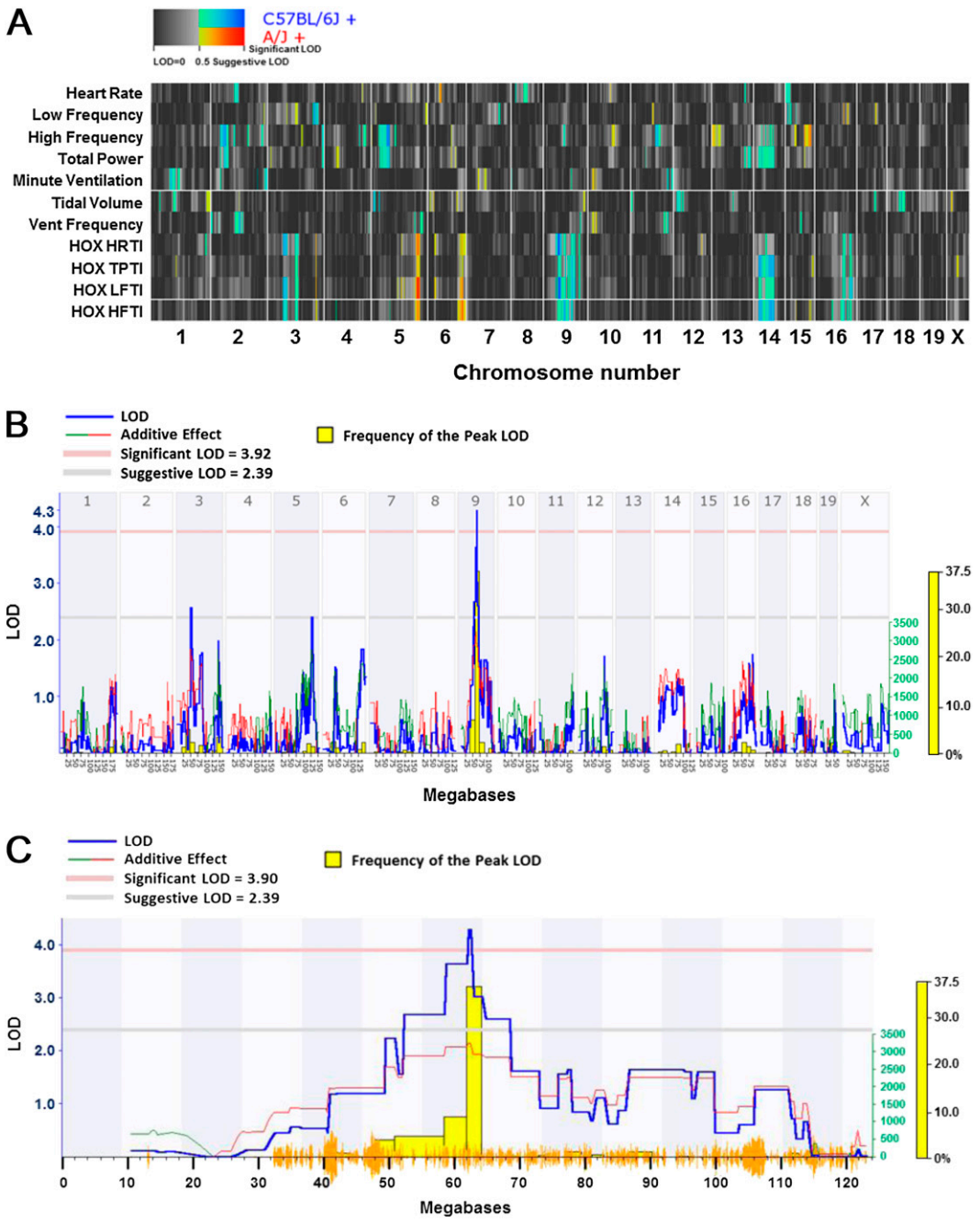

Figure 7. Genome-wide linkage maps for ventilatory, HR, and HRV phenotypes in 27 AXB/BXA RI strains of mice. (*A*) Cluster quantitative trait loci (QTL) map to identify common and unique linkages for ventilatory, HR, and HRV phenotypes in the RI strains. The *x axis* represents all of the autosomal chromosomes and the X chromosome. The *top seven rows* (*y axis*) are the basal HR, HRV, and ventilatory phenotypes, and the *bottom four rows* are the hyperoxia response phenotypes. *Yellow* to *red colors* indicate linkage strength with trait values from A/J background, and *green* to *blue colors* indicate linkage strength with trait values from C57BL/6J background. (*B*) Genome-wide linkage map for HRTI in 27 AXB/BXA RI strains of mice exposed to hyperoxia. The *x axis* represents the length of each chromosome, the *left y axis* shows the log of the odds ratio (LOD; *blue line*), and the *right y axis* shows the degree to which either A/J (*green line*) or B6 (*red line*) alleles increase phenotypic values. The numbers along the *top of the graph* indicate chromosome number. The *yellow histogram* is the frequency of the peak LOD. The *lower horizontal line* indicates suggestive linkage, and the *upper horizontal line* indicates significant ($P < 0.05$) linkage. (*C*) A detailed linkage map of chromosome 9 indicates the significant QTL for HRTI among the RI strains. *Yellow lines* on the *x axis* indicate the single-nucleotide polymorphism (SNP) density for the RI strains. *Other symbols* are as described in (*B*).

with greater HRTI and LFTI responses in RI strains homozygous for the C allele ($n = 10$ strains) compared with those with the T allele (16 strains; Table 2). This predicted amino acid substitution occurs in the TSP-1 (thrombospondin type I) repeats domain of the protein, which is responsible for cell–cell interactions, angiogenesis inhibition, and apoptosis (23).

This search strategy identified a candidate gene (hydrogen voltage-gated channel 1 [*Hvcn1*]) within the identical suggestive chromosome 5 QTLs for HRTI and LFTI. A nonsynonymous coding SNP (A/C) that causes a Glu65Ala amino acid substitution in exon 4 of *Hvcn1* significantly associated with HRTI and LFTI responses among the RI strains (Tables 1 and 2). In the suggestive chromosome 3 QTL for HRTI (Tables 1 and 2), a nonsynonymous coding SNP (C/T) in exon 1 of protocadherin 18 gene (*Pcdh18*) and an SNP (A/G) in intron 6 of the gene for solute carrier family 7, member 11 (*Slc7a11*) were in complete linkage disequilibrium, and associated significantly with differential susceptibility to hyperoxia-induced changes in HR in the RI strains. No suggestive or significant QTLs were found for other hyperoxia response phenotypes.

DISCUSSION

Numerous studies have assessed the effect of chronic hyperoxia on the lung. Pulmonary protein hyperpermeability increases in highly sensitive strains from 48 hours of hyperoxia, as seen in the current (Figure 2) and previous studies (3). However, the most significant changes in protein edema, inflammation, and histopathology were not found until 60 hours in the most susceptible strain, and later in most strains. We also found strain-dependent, hyperoxia-induced changes in $\dot{V}_E$; the earliest decline in $\dot{V}_E$ began in susceptible B6 mice at 53 hours of hyperoxia (Figure 1C). It is not clear if the precipitous reduction in $\dot{V}_E$ was a consequence of lung injury or of changes in autonomic regulation of the pulmonary system.

TABLE 1. QUANTITATIVE TRAIT LOCI FOR HEART RATE TIME INDEX AND LOW-FREQUENCY TIME INDEX PHENOTYPES IDENTIFIED BY INTERVAL MAPPING IN AXB AND BXA RECOMBINANT INBRED STRAINS EXPOSED TO HYPEROXIA

Phenotype	QTL Type	Chromosome	Marker*	Location, Mbp*	LOD†	*P* Value	Additive Effect‡
HRTI	Suggestive	3	rs3691363	47.860167	2.579	0.0705	−2759.732
			rs13477106	50.925957			
	Suggestive	5	rs3655477	122.401278	2.403	0.0829	2751.909
			rs13478527	129.764758			
	Significant	9	rs3723670	52.322901	4.298	0.0134	−3249.863
			rs3655098	68.496532			
LFTI	Suggestive	5	rs3671202	125.290217	2.632	0.0671	8.162
			rs13478527	129764758			
	Significant	9	rs4227700	58.724841	3.346	0.0340	−8.562
			rs3655098	68.496532			

Definition of abbreviations: HRTI, heart rate time index; LFTI, low-frequency time index; LOD, log of the odds ratio; Mbp, megabase pairs; QTL, quantitative trait loci; rs, RefSNP accession number.

* Markers and their locations are the proximal and distal ends of the QTL; markers outside of the QTL do not reach suggestive significance.

† Peak LOD scores for the QTL.

‡ Additive effect indicates which strain alleles increase the trait value: positive additive effect indicates that A/J alleles increase the trait value; negative additive effect indicates that C57BL/6J alleles increase trait value.

Short-term changes in parasympathetic activity during hyperbaric hyperoxia have been reported previously (17). However, there are no reports regarding the long-term implications of oxygen exposure on parasympathetic regulation of breathing.

This is the first study to describe HRV responses to continuous hyperoxia exposure in laboratory animals. Marked reductions in HR and HRV were found after 50 hours of exposure among the inbred strains (Figures 1B and 4). The changes in HR began approximately 3 hours before changes in $\dot{V}_E$ (Figure 1C). HR and HF HRV declined in a similar manner to $\dot{V}_E$, suggesting an interaction between cardiac and pulmonary responses to hyperoxia, resulting in marked decline in pulmonary function, preceded by a severely bradycardic HR that was coupled with a loss of HRV in the HF range. Differential cardiac responses, including HR and HRV susceptibility to long-term hyperoxia exposure, have not yet received attention. When conscious dogs were exposed to hyperoxia for 72 hours, increases in systemic vascular resistance were found, but cardiac output (CO) was maintained (9). It is reasonable to suggest a reduction in stroke volume in the presence of increases in systemic vascular resistance, and therefore HR must have increased to maintain CO, which is contradictory to the present results. Conversely, 24–36 hours of hyperoxia, followed by 3 hours of room air breathing, using anesthetized rabbits caused lung edema, a small decrease in HR, and a substantial increase in CO (8), although it is possible that the anesthesia affected the responses. These studies illustrate the current confusion with regard to the cardiovascular responses to chronic hyperoxia exposure.

Common symptoms in patients with acute respiratory distress syndrome include increases in lung edema and pulmonary artery pressure, accompanied by declining arterial oxygen partial pressure and systemic hypoxia (18). Our study demonstrated small, but significant, increases in lung protein content, a marker for lung edema, and histopathological evidence for alveolar damage and edema in the more susceptible hyperoxia-exposed strains after 48 hours of hyperoxia (B6, A/J, and D2). Increases in the magnitude of lung edema and alveolar damage responses to hyperoxia may have led to progressive systemic hypoxia. Hypoxemia is well known to cause bradycardia, and substantial reductions of approximately 35% in HR were reported in chickens when breathing air containing 10% oxygen (19). Furthermore, bradycardia in response to hypoxia, as opposed to tachycardia, was reported to be dependent on the absence of reflexes associated with pulmonary inflation (20). Therefore, the changes in $\dot{V}_E$ in this study (Figure 1A) suggest that declining pulmonary function, with accompanying edema (Figure 2A) and systemic hypoxemia, may have contributed to the bradycardia observed. Such a reduction in HR during hyperoxia could be a predictive tool for risk of lung injury development, although further study is required to demonstrate this characteristic of responses to hyperoxia. However, if HR and HRV responses to hyperoxia are dependent on the development of lung injury, they still have the potential, along with $\dot{V}_E$, to be useful phenotypes as indicators of the severity of lung injury.

In this study, linkage analysis identified a significant QTL on chromosome 9 for HRTI and LFTI that contains two candidate susceptibility genes, *Tipin* and *Thsd4*. *Tipin* codes for a protein

TABLE 2. CANDIDATE GENES LOCATED WITH SIGNIFICANT (CHROMOSOME 9) AND SUGGESTIVE (CHROMOSOMES 3 AND 5) QUANTITATIVE TRAIT LOCI FOR HEART RATE TIME INDEX AND LOW-FREQUENCY TIME INDEX IN AXB/BXA RECOMBINANT INBRED STRAINS OF MICE

		SNPs				RI HRTI*			RI LFTI*		
QTL	Gene	rs No.	Location (*Mbp*)	Effect	AA Change	A/J Allele	B6 Allele	*P* Value	A/J Allele	B6 Allele	*P* Value
3	*Slc7a11*	3,022,958	50.205964	A/G	†	17,209 (766)	11,180 (1,162)	0.014	44.71 (2.50)	32.73 (4.07)	<0.001
5	*Hvcn1*	13,478,496	122.683604	A/C	Glu65Ala	11,358 (1,461)	16,192 (890)	0.010	30.85 (3.38)	43.51 (2.75)	0.018
9	*Thsd4*	6,224,703	59.835173	C/T	Met770Val	18,417 (827)	12,686 (962)	<0.001	48.57 (3.18)	34.81 (2.74)	0.004
	Tipin	13,459,109	64.152234	G/T	Cys265Phe	18,201 (822)	12,820 (1,014)	0.001	49.86 (3.27)	34.00 (2.39)	<0.001

Definition of abbreviations: HRTI, heart rate time index; *Hvcn1*, hydrogen voltage-gated channel 1; LFTI, low-frequency time index; LOD, log of the odds ratio; Mbp, megabase pairs; QTL, quantitative trait loci; RI, recombinant inbred; rs, RefSNP accession number; *Slc7a11*, solute carrier family 7, member11; SNPs, single-nucleotide polymorphisms; *Thsd4*, thrombospondin type I, domain containing 4; *Tipin*, timeless interacting protein.

* Mean (SEM).

† Intron SNP.

that complexes with another protein, TIMELESS, to interact with components of DNA replication under normal and genotoxic stress conditions (21, 22). We found that RI strains with a nonsynonymous coding SNP in exon 8 of *Tipin* had significantly lower HRTI and LFTI (i.e., more susceptible phenotypes) compared with those strains with the wild-type allele which supports a potential role for this gene in HR and HRV responses to hyperoxia. Another candidate gene in the chromosome 9 QTL, *Thsd4*, has not been well studied. However, a recent investigation of mouse *Adamtsl6* (a disintegrin and metalloproteinase with thrombospondin motifs–like 6; a synonym for *Thsd4*) found that the protein binds directly to fibrillin-1, promoting fibrillin-1 matrix assembly in a number of tissues, including heart (23). Human *ADAMTSL6* has been identified as a candidate gene associated with fibrillinopathies, and may contribute to cardiac valvular anomalies (24), including mitral valve prolapse (25), which may only present under conditions of cardiovascular stress. Interestingly, the human homolog, *THSD4*, has been identified as a significant candidate gene in a genome-wide association study of lung function (26). As with *Tipin*, a nonsynonymous coding SNP in *Thsd4* associated significantly with enhanced HRTI and LFTI after hyperoxia, supporting a potential role for *Thsd4* in this model.

A suggestive QTL on chromosome 5 was found in common for HRTI and LFTI, which contained a candidate gene, *Hvcn1*. The specific mechanism through which *Hvcn1* might contribute to hyperoxia phenotypes is not clear, although it is postulated that loss of HVCN1 function may reduce mucosal acidification and prevent epithelial injury induced by oxidant stress (27). *Slc7a11* is a candidate gene in the suggestive QTL on chromosome 3 that has an SNP that associated with differential HRTI and LFTI responses to hyperoxia. *Slc7a11* codes the protein, xCT, which is up-regulated after exposure to hyperoxia (28), and is regulated in part by *Nrf2*, which has an important protective role in hyperoxia-induced ALI (6, 29). The antioxidant and anti-inflammatory properties of *Slc7a11* warrant continued investigation in this model.

It is important to note that the QTLs and candidate genes for hyperoxia-induced changes in HR and HRV have not previously been associated with other hyperoxia-induced cardiopulmonary phenotypes. Cho and colleagues (4) identified a significant QTL on chromosome 2 and a suggestive QTL on chromosome 3 (different from the present study), for lung inflammation of permeability phenotypes. In a model of mortality caused by hyperoxia-induced ALI, Prows and colleagues (30) found highly significant QTLs on chromosomes 1 (*Shali1*, 54–68 Mbp), 4 (*Shali2*, 104 Mbp to distal end), 9 (*Shali4*, 88 Mbp to distal end), and 15 (*Shali3*, 0–50 Mbp); a significant QTL was found on chromosome 1 (*Shali5*, 140 Mbp to distal end). Interestingly, no studies identified common QTLs for hyperoxia-induced lung injury, mortality, or HRV phenotypes. Lack of concordance between hyperoxia response QTLs illustrates the great complexity of cardiopulmonary responses to oxidant exposure, and suggests that different susceptibility genes and mechanisms are likely important in determining the various hyperoxia responses.

In conclusion, we first reported significant and possibly debilitating reductions in HR and HRV during hyperoxia exposure in inbred mice. Next, we found significant and suggestive QTLs in a panel of AXBXA RI strains. SNPs in candidate genes *Tipin* and *Thsd4* significantly associated with differential HRTI and LFTI responses to hyperoxia in the RI strains, suggesting their potential roles in determining oxidant-induced changes in HR and HRV. Hyperoxia-induced changes in HR and HRV may be useful indicators of ALI in mice that may be monitored temporally.

Author disclosures are available with the text of this article at www.atsjournals.org.

Acknowledgments: The authors thank Drs. Donald N. Cook and Lauranell H. Burch for critical review of the manuscript.

References

1. Janssen YM, Van Houten B, Borm PJ, Mossman BT. Cell and tissue responses to oxidative damage. *Lab Invest* 1993;69:261–274.
2. Bhandari V, Gruen JR. The genetics of bronchopulmonary dysplasia. *Semin Perinatol* 2006;30:185–191.
3. Hudak BB, Zhang LY, Kleeberger SR. Inter-strain variation in susceptibility to hyperoxic injury of murine airways. *Pharmacogenetics* 1993;3:135–143.
4. Cho HY, Jedlicka AE, Reddy SP, Zhang LY, Kensler TW, Kleeberger SR. Linkage analysis of susceptibility to hyperoxia: Nrf2 is a candidate gene. *Am J Respir Cell Mol Biol* 2002;26:42–51.
5. Crapo JD, Barry BE, Chang LY, Mercer RR. Alterations in lung structure caused by inhalation of oxidants. *J Toxicol Environ Health* 1984;13:301–321.
6. Cho HY, Jedlicka AE, Reddy SP, Kensler TW, Yamamoto M, Zhang LY, Kleeberger SR. Role of Nrf2 in protection against hyperoxic lung injury in mice. *Am J Respir Cell Mol Biol* 2002;26:175–182.
7. Cho HY, Reddy SP, Kleeberger SR. Nrf2 defends the lung from oxidative stress. *Antioxid Redox Signal* 2006;8:76–87.
8. Beran AV, Sperling DR, Huxtable RF. Cardiopulmonary changes following 24–36 hours of hyperoxia. *Aviat Space Environ Med* 1975;46: 419–422.
9. Moran JF, Wolfe WG. Hemodynamic effects of prolonged hyperoxia. *Ann Surg* 1978;187:73–78.
10. De Burgh Daly M. Interactions between respiration and circulation. In: Cherniack NS, Widdicombe JG, editors. The respiratory system. Bethesda, MD: American Physiological Society; 1986. pp. 529–594.
11. Taylor BL, Zhulin IB. Pas domains: internal sensors of oxygen, redox potential, and light. *Microbiol Mol Biol Rev* 1999;63:479–506.
12. Demling R, Lalonde C, Youn YK, Picard L. Effect of graded increases in smoke inhalation injury on the early systemic response to a body burn. *Crit Care Med* 1995;23:171–178.
13. Sventek JC, Zambraski EJ. Effects of chronic hyperoxia on the cardiovascular responses to vasoactive compounds in the rabbit. *Aviat Space Environ Med* 1988;59:314–320.
14. Abildstrom SZ, Jensen BT, Agner E, Torp-Pedersen C, Nyvad O, Wachtell K, Ottesen MM, Kanters JK. Heart rate versus heart rate variability in risk prediction after myocardial infarction. *J Cardiovasc Electrophysiol* 2003;14:168–173.
15. Howden R, Liu E, Miller-DeGraff L, Keener HL, Walker C, Clark JA, Myers PH, Rouse DC, Wiltshire T, Kleeberger SR. The genetic contribution to heart rate and heart rate variability in quiescent mice. *Am J Physiol Heart Circ Physiol* 2008;295:H59–H68.
16. Wang J, Williams RW, Manly KF. WebQTL: Web-based complex trait analysis. *Neuroinformatics* 2003;1:299–308.
17. Lund VE, Kentala E, Scheinin H, Klossner J, Helenius H, Sariola-Heinonen K, Jalonen J. Heart rate variability in healthy volunteers during normobaric and hyperbaric hyperoxia. *Acta Physiol Scand* 1999;167:29–35.
18. Piantadosi CA, Schwartz DA. The acute respiratory distress syndrome. *Ann Intern Med* 2004;141:460–470.
19. Butler PJ. Effect of progressive hypoxia on the respiratory and cardiovascular system of chickens. *J Physiol* 1967;191:309–324.
20. Daly MD, Hazzledine JL. The effects of artificially induced hyperventilation on the primary cardiac reflex response to stimulation of the carotid bodies in the dog. *J Physiol* 1963;168:872–889.
21. Chou DM, Elledge SJ. Tipin and Timeless form a mutually protective complex required for genotoxic stress resistance and checkpoint function. *Proc Natl Acad Sci USA* 2006;103:18143–18147.
22. Kondratov RV, Antoch MP. Circadian proteins in the regulation of cell cycle and genotoxic stress responses. *Trends Cell Biol* 2007;17: 311–317.
23. Tsutsui K, Manabe R, Yamada T, Nakano I, Oguri Y, Keene DR, Sengle G, Sakai LY, Sekiguchi K. ADAMTSL-6 is a novel extracellular matrix protein that binds to fibrillin-1 and promotes fibrillin-1 fibril formation. *J Biol Chem* 2010;285:4870–4882.
24. Le Goff C, Morice-Picard F, Dagoneau N, Wang LW, Perrot C, Crow YJ, Bauer F, Flori E, Prost-Squarcioni C, Krakow D, *et al.* ADAMTSL2

mutations in geleophysic dysplasia demonstrate a role for adamts-like proteins in TGF-beta bioavailability regulation. *Nat Genet* 2008;40:1119–1123.
25. Weyman AE, Scherrer-Crosbie M. Marfan syndrome and mitral valve prolapse. *J Clin Invest* 2004;114:1543–1546.
26. Repapi E, Sayers I, Wain LV, Burton PR, Johnson T, Obeidat M, Zhao JH, Ramasamy A, Zhai G, Vitart V, *et al*. Genome-wide association study identifies five loci associated with lung function. *Nat Genet* 42; 42:36–44.
27. Capasso M, Bhamrah MK, Henley T, Boyd RS, Langlais C, Cain K, Dinsdale D, Pulford K, Khan M, Musset B, *et al*. HVCN1 modulates BCR signal strength via regulation of BCR-dependent generation of reactive oxygen species. *Nat Immunol* 2010;11:265–272.
28. Bannai S, Sato H, Ishii T, Sugita Y. Induction of cystine transport activity in human fibroblasts by oxygen. *J Biol Chem* 1989;264:18480–18484.
29. Lewerenz J, Albrecht P, Tien ML, Henke N, Karumbayaram S, Kornblum HI, Wiedau-Pazos M, Schubert D, Maher P, Methner A. Induction of Nrf2 and xCT are involved in the action of the neuroprotective antibiotic ceftriaxone *in vitro*. *J Neurochem* 2009;111:332–343.
30. Prows DR, Winterberg AV, Gibbons WJ Jr, Burzynski BB, Liu C, Nick TG. Reciprocal backcross mice confirm major loci linked to hyperoxic acute lung injury survival time. *Physiol Genomics* 2009;38:158–168.